










Supplementary Material for:  
Precursory velocity changes prior to the 2019 paroxysms at Stromboli volcano, Italy, from coda wave interferometry

 Alexander S. Yates<sup>\*α,β,γ</sup>,  Corentin Caudron<sup>α,β,γ</sup>,  Aurélien Mordret<sup>α,δ</sup>,  Philippe Lesage<sup>α</sup>,  
 Andrea Cannata<sup>ε,ζ</sup>,  Flavio Cannavo<sup>ζ</sup>,  Thomas Lecocq<sup>η</sup>,  Virginie Pinel<sup>α</sup>, and  Lucia Zaccarelli<sup>θ</sup>

<sup>α</sup> Univ. Grenoble Alpes, Univ. Savoie Mont Blanc, CNRS, IRD, Univ. Gustave Eiffel, ISTerre, 38000 Grenoble, France.

<sup>β</sup> Laboratoire G-Time, Department of Geosciences, Environment and Society, Université libre de Bruxelles, Belgium.

<sup>γ</sup> WEL Research Institute, Avenue Pasteur, 6, 1300 Wavre, Belgium.

<sup>δ</sup> Department of Geophysics and Sedimentary Basins, GEUS, Geological Survey of Denmark and Greenland, Copenhagen, Denmark.

<sup>ε</sup> Dipartimento di Scienze Biologiche, Geologiche e Ambientali, Università degli Studi di Catania, Corso Italia 57, 95129 Catania, Italy.

<sup>ζ</sup> Istituto Nazionale di Geofisica e Vulcanologia - Sezione di Catania, Osservatorio Etneo, Piazza Roma 2, 95125 Catania, Italy.

<sup>η</sup> Seismology and Gravimetry Department, Royal Observatory of Belgium, Uccle, Belgium.

<sup>θ</sup> Istituto Nazionale di Geofisica e Vulcanologia, Sezione di Bologna, Bologna, Italy.

This supplementary material accompanies the article:

Yates, A. S., Caudron, C., Mordret, A., Lesage, P., Cannata, A., Cannavo, F., Lecocq, T., Pinel, V., and Zaccarelli, L. (2025) "Precursory velocity changes prior to the 2019 paroxysms at Stromboli volcano, Italy, from coda wave interferometry", *Volcanica*, 8(1), pp. 203–223. DOI: <https://doi.org/10.30909/vol/cyrk4139>.

Yates et al. (2025) should be cited if this material is used independently of the article.

Table S1: Parameters used in config table of MSNoise. Note that `dtc_minlag` and `dtc_width`, usually defined in the config table, are instead defined within the filter table (i.e. [Table S2](#)).

name	value
<code>analysis_duration</code>	86400
<code>cc_normalisation</code>	NO
<code>cc_sampling_rate</code>	25
<code>cc_type</code>	CC
<code>cc_type_single_station_SC</code>	CC
<code>clip_after_whiten</code>	Y
<code>components_to_compute</code>	ZZ
<code>components_to_compute_single_station</code>	EN,EZ,NZ
<code>corr_duration</code>	1800
<code>dtc_lag</code>	static
<code>dtc_maxdt</code>	0.25
<code>dtc_maxerr</code>	0.1
<code>dtc_mincoh</code>	0.5
<code>dtc_sides</code>	both
<code>maxlag</code>	120
<code>mov_stack</code>	5
<code>overlap</code>	0
<code>preprocess_highpass</code>	0.01
<code>preprocess_lowpass</code>	8
<code>preprocess_max_gap</code>	10
<code>preprocess_taper_length</code>	20
<code>ref_begin</code>	2013-01-01
<code>ref_end</code>	2022-01-01
<code>resampling_method</code>	Lanczos
<code>stack_method</code>	linear
<code>stretching_max</code>	0.01
<code>stretching_nsteps</code>	1000
<code>whitening</code>	A
<code>whitening_type</code>	B
<code>windsorizing</code>	3

Table S2: Parameters used in filter table of MSNoise. Note, this uses a modified version where `dtc_minlag` and `dtc_width` are defined within the filter table rather than config table ([Table S1](#)).

ref	low	mwcs_low	high	mwcs_high	mwcs_wlen	mwcs_step	dtc_width	dtc_minlag
2	1.0	1.1	2.0	1.9	4.0	2.0	20.0	5.0
3	2.0	2.1	4.0	3.9	2.0	1.0	10.0	5.0
4	0.5	0.55	1.0	0.95	8.0	4.0	30.0	10.0

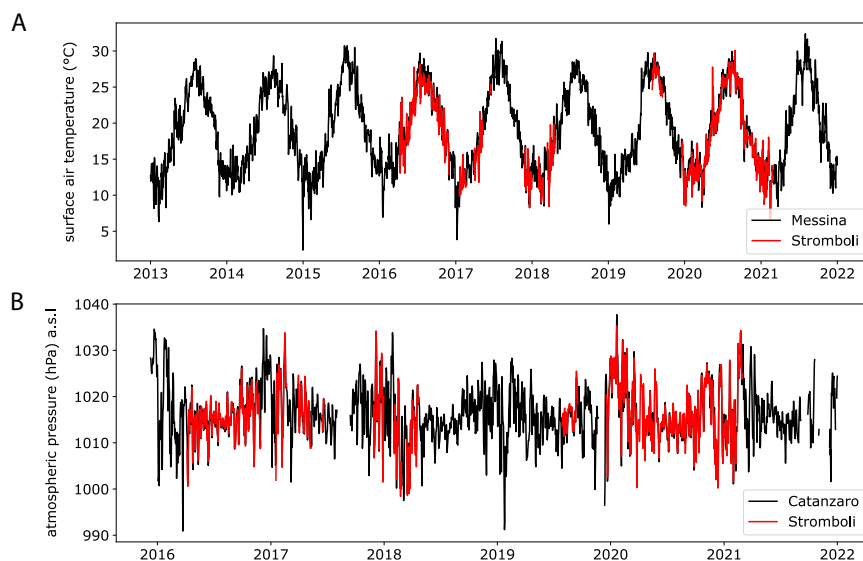


Figure S1: Comparison of surface air temperature and sea-level atmospheric pressure measurements at Stromboli with those from other meteorological stations with improved data availability (Messina for temperature measurements and Catanzaro for sea level pressure).

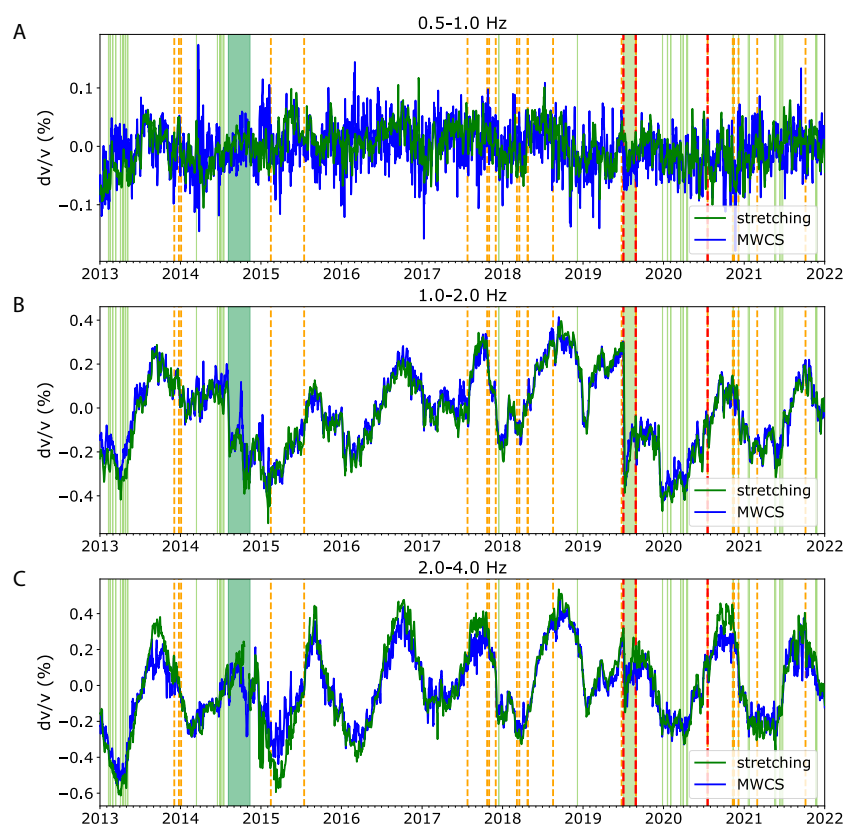


Figure S2: Velocity changes computed in three different frequency bands using moving-window cross-spectral technique (blue) and the stretching technique (green). Volcanic activity described by red-dashed-lines = paroxysms, orange-dashed-lines = major explosions, light-green-shading = lava flows, dark-green shading = 2014 flank eruption. [A] 0.5–1.0 Hz. [B] 1.0–2.0 Hz. [C] 2.0–4.0 Hz.

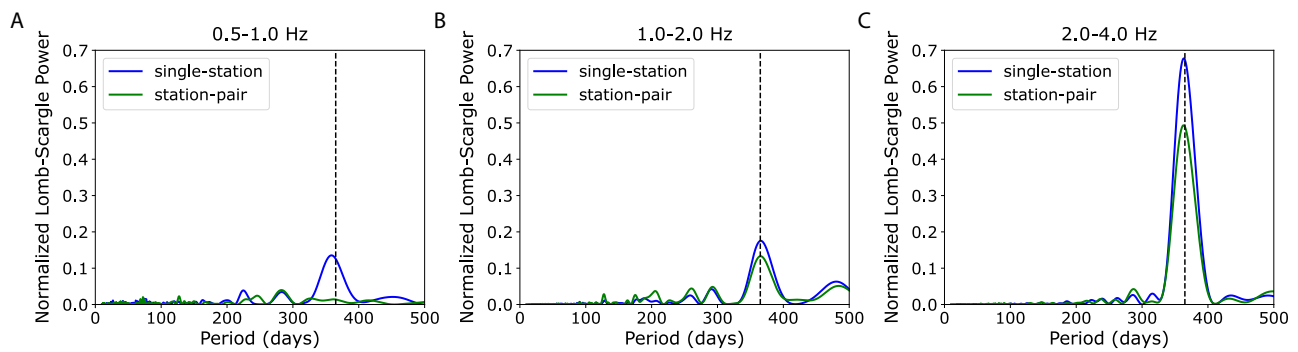


Figure S3: Spectra of velocity changes (stretching technique) at different frequencies visualized through application of Lomb-Scargle periodogram [Lomb 1976; Gherghetta and Pomarol 2000]. This fits a range of sinusoids with different frequencies to a given signal, returning a unitless power that reflects the goodness of fit. We use the open source Python package SciPy [Virtanen et al. 2020] for this (`scipy.signal.lombscargle` function), outputting the normalized power. With this, the computed periodogram is normalized by the residuals of the data around a constant baseline (at zero). Vertical-dashed black line indicates 365-day (annual) period. [A] 0.5–1.0 Hz. [B] 1.0–2.0 Hz. [C] 2.0–4.0 Hz.

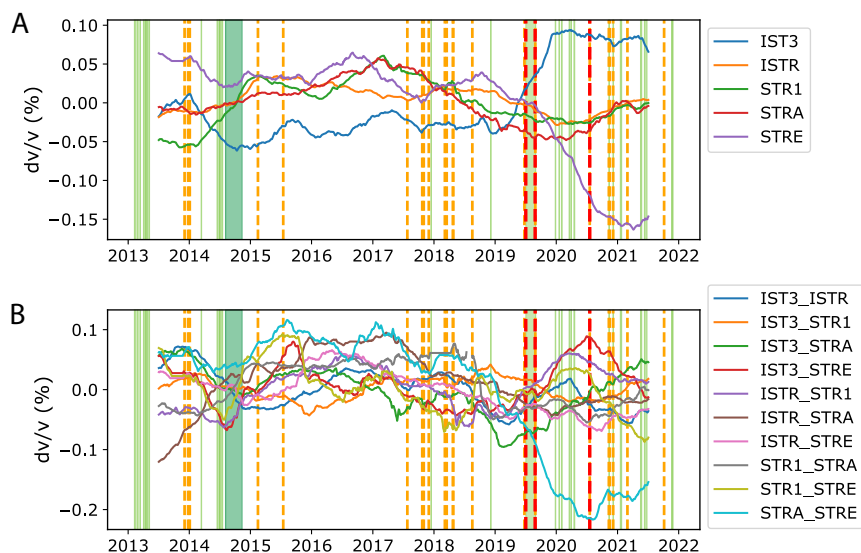


Figure S4: Long-term 0.5–1.0 Hz velocity changes (365-day smoothing, stretching technique) for [A] individual single-stations and [B] individual station pairs. Volcanic activity described by red-dashed-lines = paroxysms, orange-dashed-lines = major explosions, light-green-shading = lava flows, dark-green shading = 2014 flank eruption.

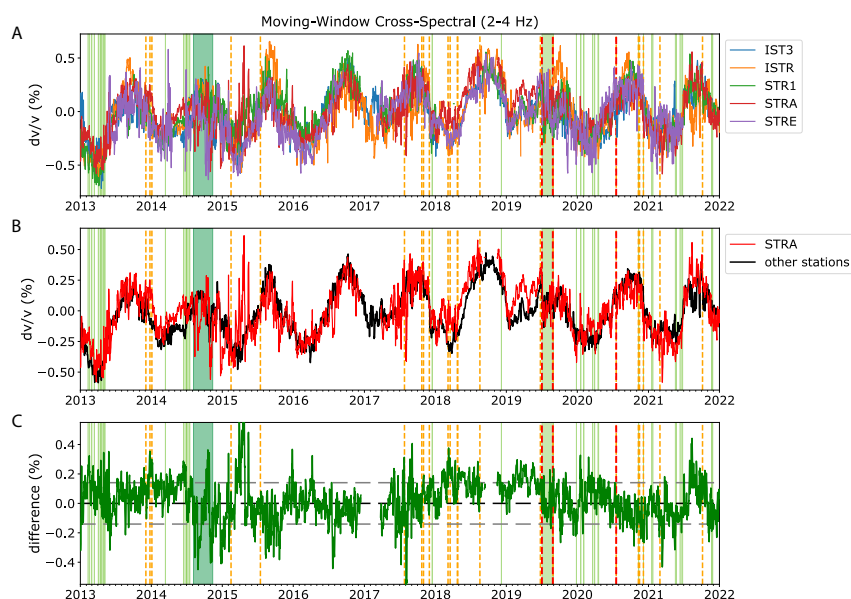


Figure S5: Comparing 2.0–4.0 Hz velocities (using moving-window cross-spectral technique) recorded at STRA station with other four stations. Volcanic activity described by red-dashed-lines = paroxysms, orange-dashed-lines = major explosions, light-green-shading = lava flows, dark-green shading = 2014 flank eruption. [A] Single-station seismic velocities for all stations. [B] Velocities for STRA station compared with average of IST3, ISTR, STR1, and STRE stations. [C] Difference between average velocity of STRA and other four stations. Grey dashed-lines represent one standard deviation of all calculated differences over the nine years either side of zero (black dashed-line).

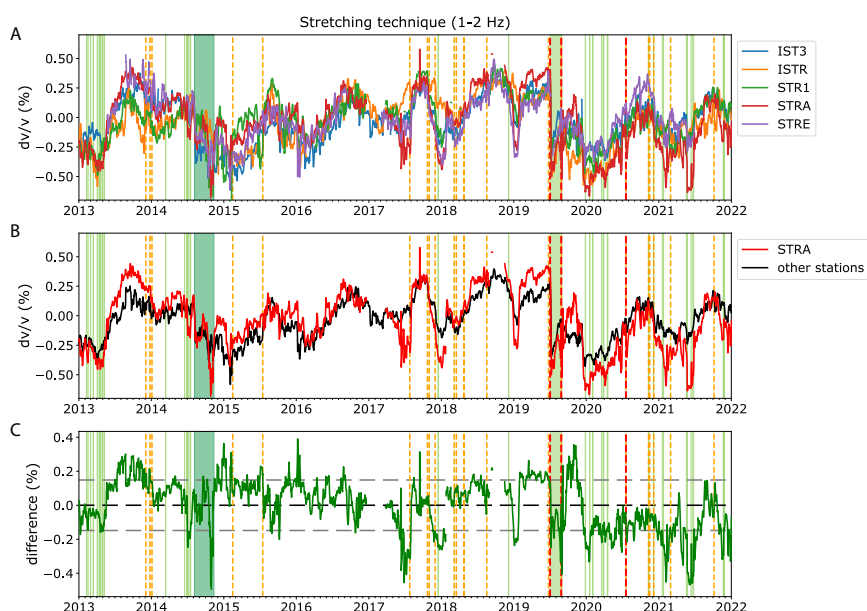


Figure S6: Comparing 1.0–2.0 Hz velocities (stretching technique) recorded at STRA station with other four stations. Volcanic activity described by red-dashed-lines = paroxysms, orange-dashed-lines = major explosions, light-green-shading = lava flows, dark-green shading = 2014 flank eruption. [A] Single-station seismic velocities for all stations. [B] Velocities for STRA station compared with average of IST3, ISTR, STR1, and STRE stations. [C] Difference between average velocity of STRA and other four stations. Grey dashed-lines represent one standard deviation of all calculated differences over the nine years either side of zero (black dashed-line).

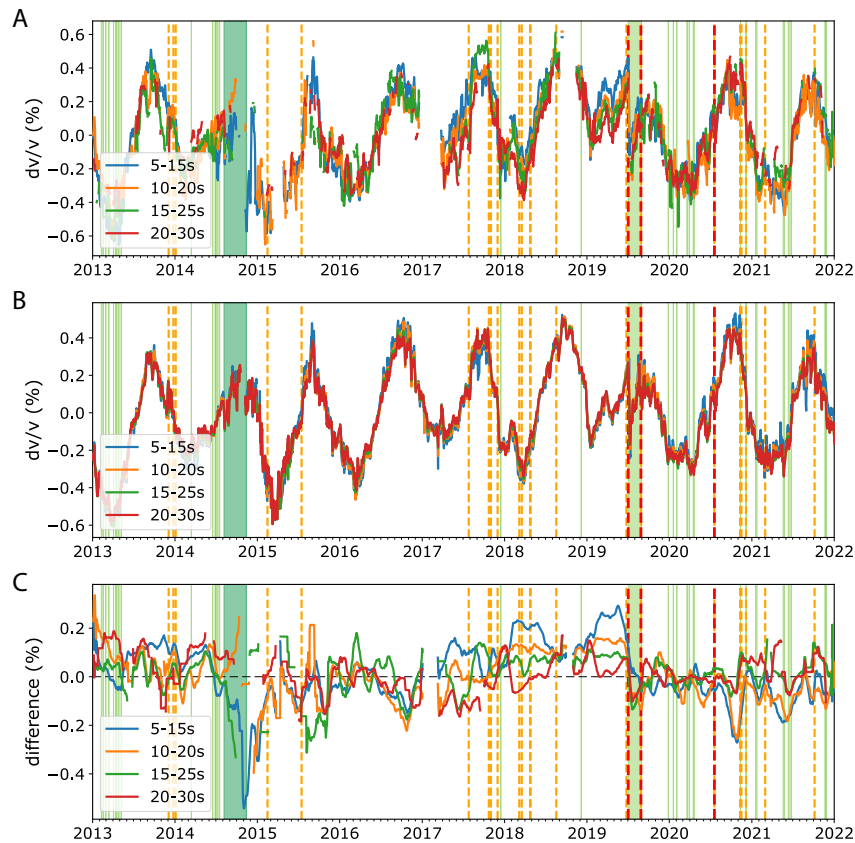


Figure S7: Comparing velocities measured at STRA station and all other stations at different lag times in the coda. Volcanic activity described by red-dashed-lines = paroxysms, orange-dashed-lines = major explosions, light-green-shading = lava flows, dark-green shading = 2014 flank eruption. [A] Velocity changes at STRA station. [B] Average of velocity changes at IST3, ISTR, STR1, STRE stations. [C] difference between STRA and average of other stations.

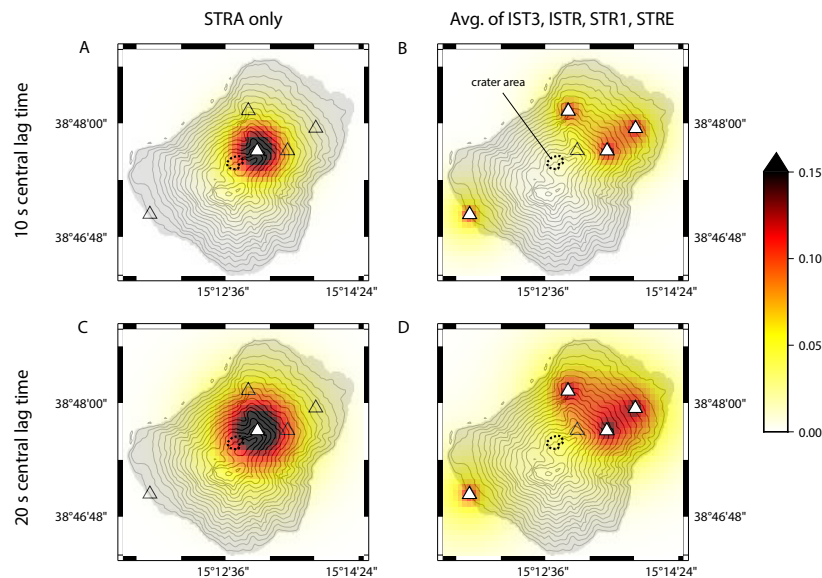


Figure S8: Comparison between lateral sensitivity kernels computed using 10 s central lag time and sensitivity kernels using 20 s central lag time. In each subplot, only contributing stations (triangles) are filled (white). [A] STRA station sensitivity, 10 s central lag time. [B] combined sensitivity of IST3, ISTR, STR1, STRE stations, 10 s central lag time. [C] STRA station sensitivity, 20 s central lag time. [D] combined sensitivity of IST3, ISTR, STR1, STRE stations, 20 s central lag time.

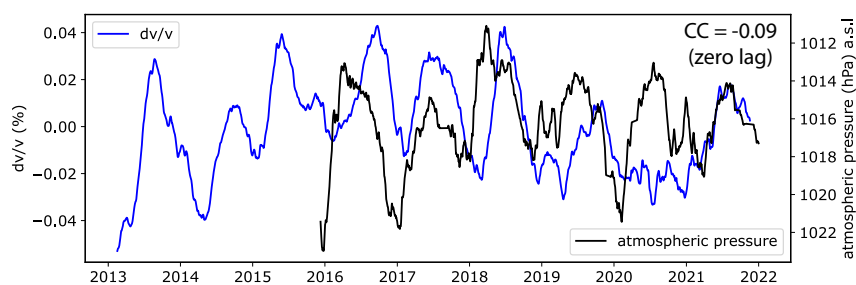


Figure S9: Single-station velocity changes at 0.5–1.0 Hz (blue-line) compared atmospheric pressure changes (both smoothed by 90 days). The zero-lag correlation coefficient is also computed ( $CC = -0.09$ ) at this smoothing. With no smoothing, the absolute value of the correlation coefficient falls below 0.01.

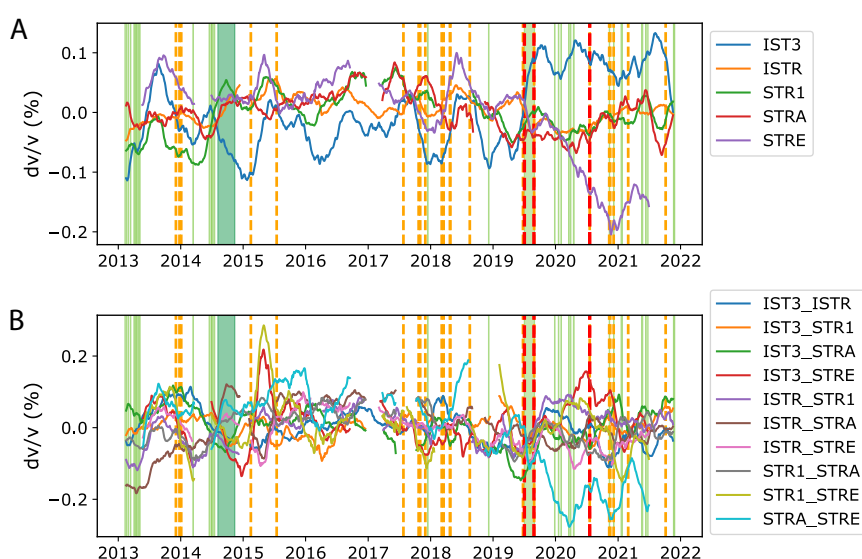


Figure S10: Long-term 0.5–1.0 Hz velocity changes (90-day smoothing, stretching technique) for [A] individual single-stations and [B] individual station pairs. Volcanic activity described by red-dashed-lines = paroxysms, orange-dashed-lines = major explosions, light-green-shading = lava flows, dark-green shading = 2014 flank eruption.

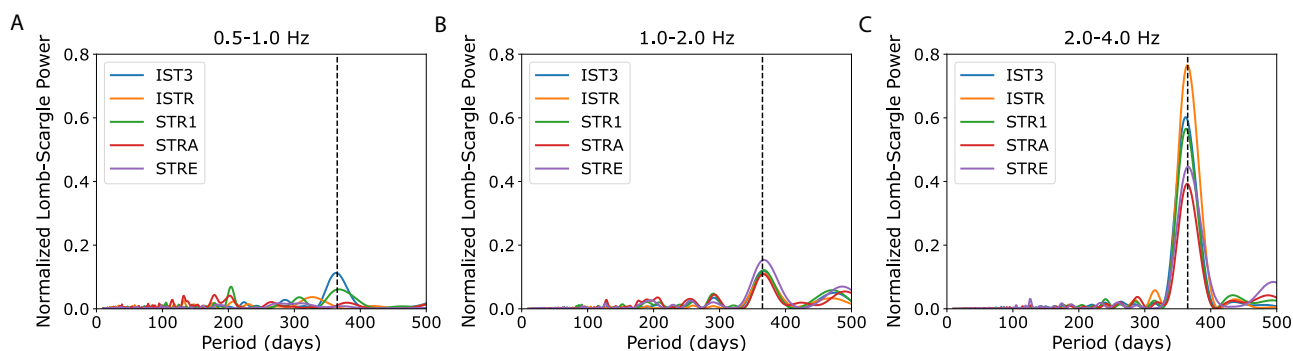


Figure S11: Spectra of velocity changes (stretching technique) at different frequencies for different single-station, visualized through application of Lomb-Scargle Periodogram [Lomb 1976; Gherghetta and Pomarol 2000]. See Figure S3 caption for additional details on normalized power output. Vertical-dashed black line indicates 365-day (annual) period. [A] 0.5–1.0 Hz. [B] 1.0–2.0 Hz. [C] 2.0–4.0 Hz.

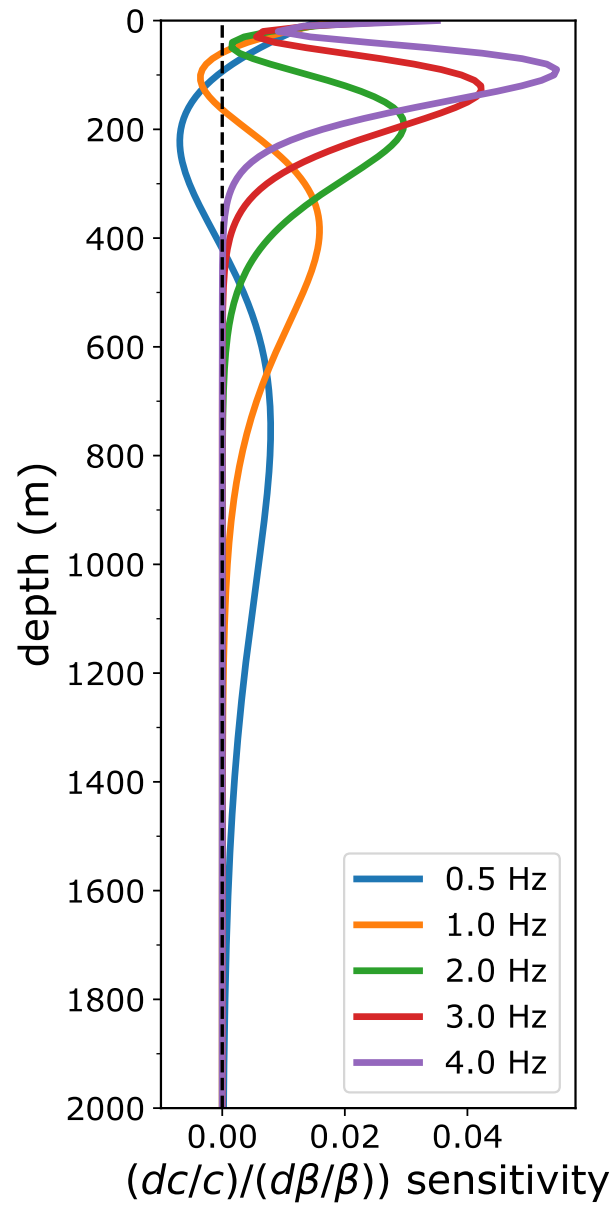


Figure S12: Sensitivity kernels for Rayleigh waves between 0.5–4.0 Hz.  $dc/c$  represents relative change in Rayleigh wave phase velocity and  $d\beta/\beta$  the relative change in shear wave velocity. Velocity model consists of linearly increasing velocities from  $V_s = 670 \text{ m s}^{-1}$  at the surface (corresponding to average shear-wave velocity in upper 100 m from [Chouet et al. \[1998\]](#)) to  $2500 \text{ m s}^{-1}$  at 2 km depth (corresponding approximately to the models of [La Rocca et al. \[2004\]](#)).



## COPYRIGHT

© The Author(s) 2025. This article is distributed under the terms of the [Creative Commons Attribution 4.0 International License](#), which permits unrestricted use, distribution, and reproduction in any medium, provided you give appropriate credit to the original author(s) and the source, provide a link to the Creative Commons license, and indicate if changes were made.

## REFERENCES

- Chouet, B., G. De Luca, G. Milana, P. Dawson, M. Martini, and R. Scarpa (1998). “Shallow velocity structure of Stromboli Volcano, Italy, derived from small-aperture array measurements of Strombolian tremor”. In: *Bulletin of the Seismological Society of America* 88(3), pages 653–666. DOI: [10.1785/bssa0880030653](#).
- Gherghetta, T. and A. Pomarol (2000). “Bulk fields and supersymmetry in a slice of AdS”. In: *Nuclear Physics B* 586(1-2), pages 141–162. DOI: [10.1016/S0550-3213\(00\)00392-8](#).
- La Rocca, M., G. Saccorotti, E. Del Pezzo, and J. Ibanez (2004). “Probabilistic source location of explosion quakes at Stromboli volcano estimated with double array data”. In: *Journal of Volcanology and Geothermal Research* 131(1-2), pages 123–142. DOI: [10.1016/S0377-0273\(03\)00321-4](#).
- Lomb, N. R. (1976). “Least-squares frequency analysis of unequally spaced data”. In: *Astrophysics and Space Science* 39(2), pages 447–462. DOI: [10.1007/BF00648343](#).
- Virtanen, P., R. Gommers, T. E. Oliphant, M. Haberland, T. Reddy, D. Cournapeau, E. Burovski, P. Peterson, W. Weckesser, J. Bright, S. J. van der Walt, M. Brett, J. Wilson, K. J. Millman, N. Mayorov, A. R. Nelson, E. Jones, R. Kern, E. Larson, C. J. Carey, Í. Polat, ..., and Y. Vázquez-Baeza (2020). “SciPy 1.0: fundamental algorithms for scientific computing in Python”. In: *Nature Methods* 17(3), pages 261–272. DOI: [10.1038/s41592-019-0686-2](#).